

COMPARISON OF TES FFSM EDDIES AND MOC STORMS, MY 24–26

John Noble, *San Jose State University, NASA Ames Research Center*

R. J. Wilson, *NOAA, Geophysical Fluid Dynamics Laboratory*

R. M. Haberle, *NASA Ames Research Center*

J. R. Barnes, *Oregon State University*

J. L. Hollingsworth, *NASA Ames Research Center*

M. A. Kahre, *NASA Ames Research Center*

A. F. C. Bridger, *San Jose State University, NASA Ames Research Center*

B. A. Cantor, *Malin Space Science System*

Fourth International Workshop on the Mars Atmosphere
February 8-11, 2011, Paris, France

Datasets

- Thermal Emission Spectrometer (TES) temperature and dust opacity (Smith)
- Mars Orbiter Camera (MOC) imagery & opacity (Malin and Cantor)
- FFSSM-filtered (Fast Fourier Synoptic Mapping) TES temperature (Barnes)

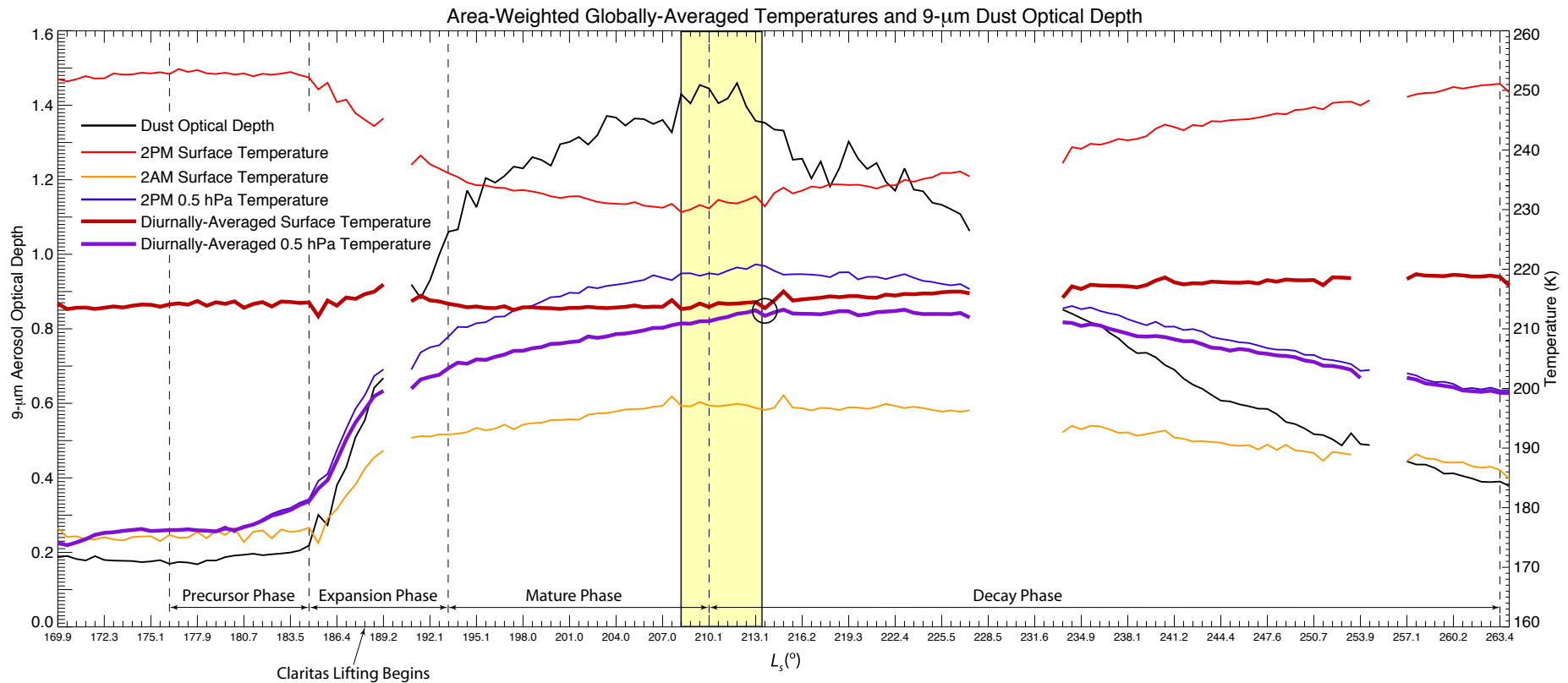
Fast Fourier Synoptic Mapping (FFSM) of TES T

- Spectral analysis method that creates synoptic maps from asynoptic data
 - Maintains full space-time resolution without distorting or smoothing higher frequency ($\sim 1-3$ sols) weather signals
 - Removes the time mean, zonal mean, and westward diurnal tide. (Barnes 2001, 2003, 2006)
- FFSM-filtered TES data show eastward-traveling waves at 60° S with a period of ~ 3 sols.
- We hypothesize that these are eastward-traveling baroclinic eddies

Objectives

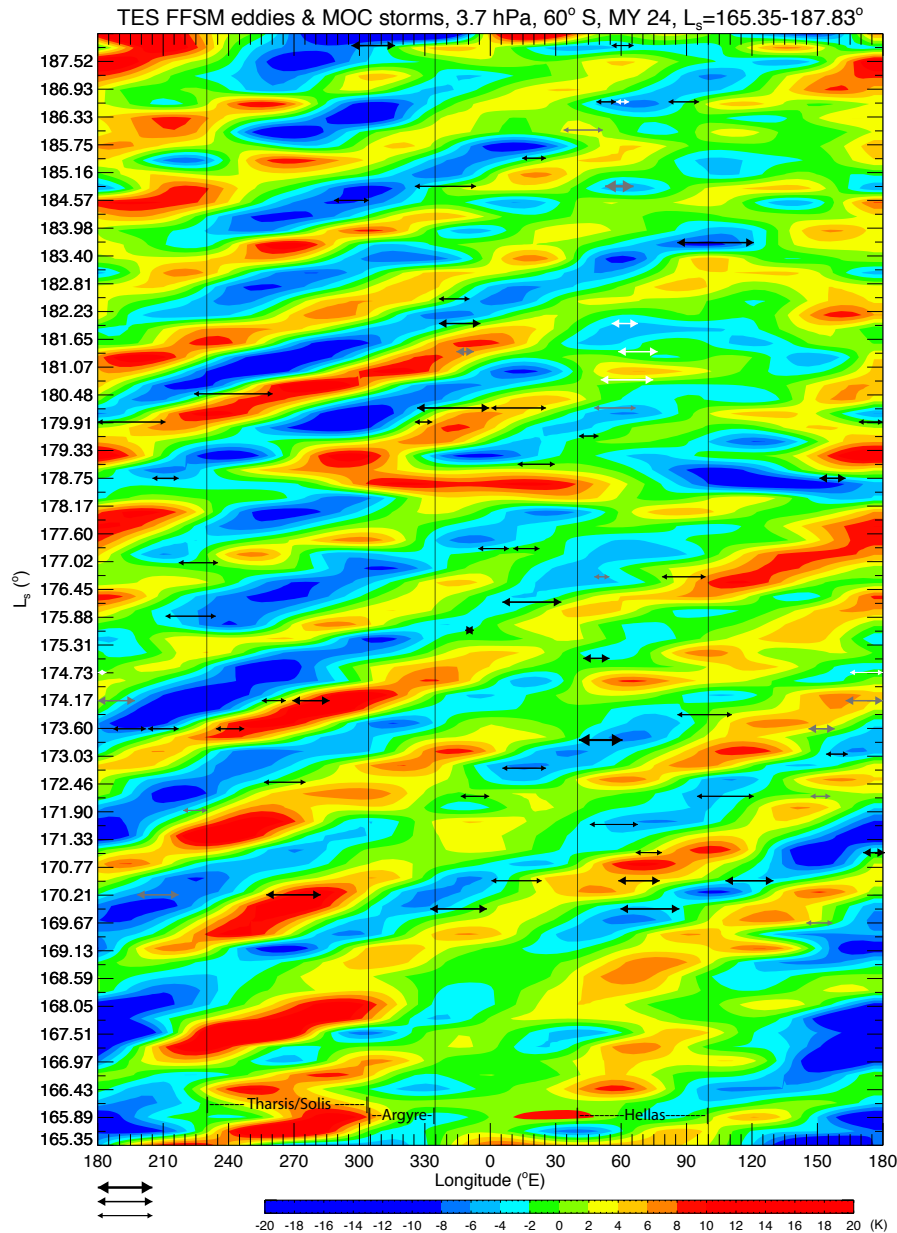
1. Integrate and examine all available MGS data
2. Better understand and characterize dust storm initiation and expansion
 - Evolution of temperature and dust opacity fields
3. Compare MOC storms with baroclinic eddies inferred from FFSSM-filtered TES temperatures

MY 25 PDS phases, TES global temperature & dust opacity



1. **Precursor:** $L_s=176.2\text{--}184.7^\circ$, storm initiation and early growth around the Hellas region
2. **Expansion:** $L_s=184.7\text{--}193^\circ$, expansion of storm activity east/northeast of Hellas, development of new lifting centers in Daedalia and Solis Plani, and storm growth to planetary-scale
3. **Mature:** $L_s=193\text{--}210^\circ$, peak of globally-averaged opacity and temperature (sfc & 0.5 hPa)
4. **Decay:** $L_s=210\text{--}263^\circ$, opacity and temperature fields return to seasonal levels

FFSM eddies and MOC storms, 60° S, 3.7 hPa, MY 24



Arrows delimit longitudinal extent of MOC visible storms;

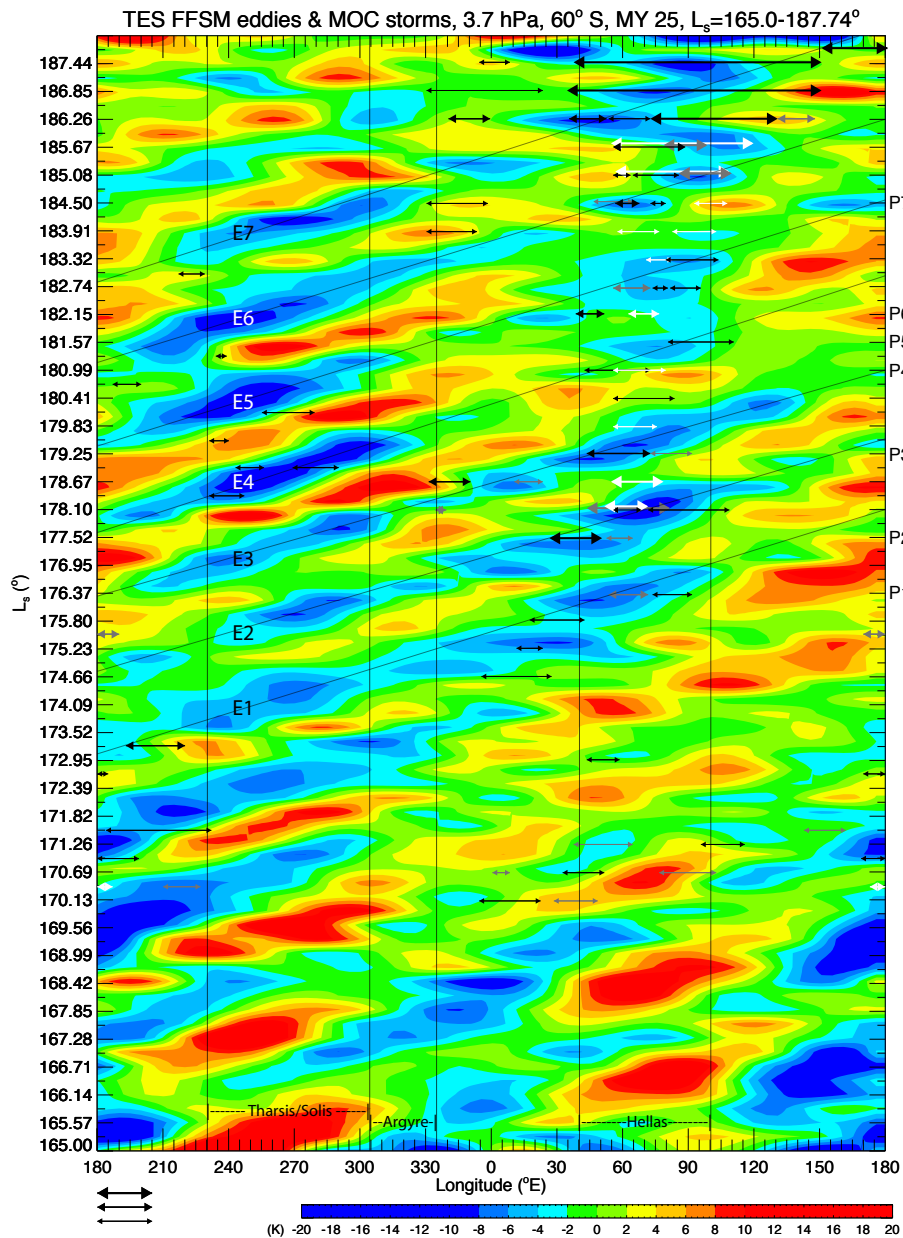
- black (< 45 S), grey (35–45 S), white (25–35 S)

- Correlation between eastward propagation of cold anomalies and eastward evolution of storms.

$L_s=170.49$ (330 and 60 E);
 $L_s=172.7$ (0 E); and
 $L_s=184.57$ (290 E).

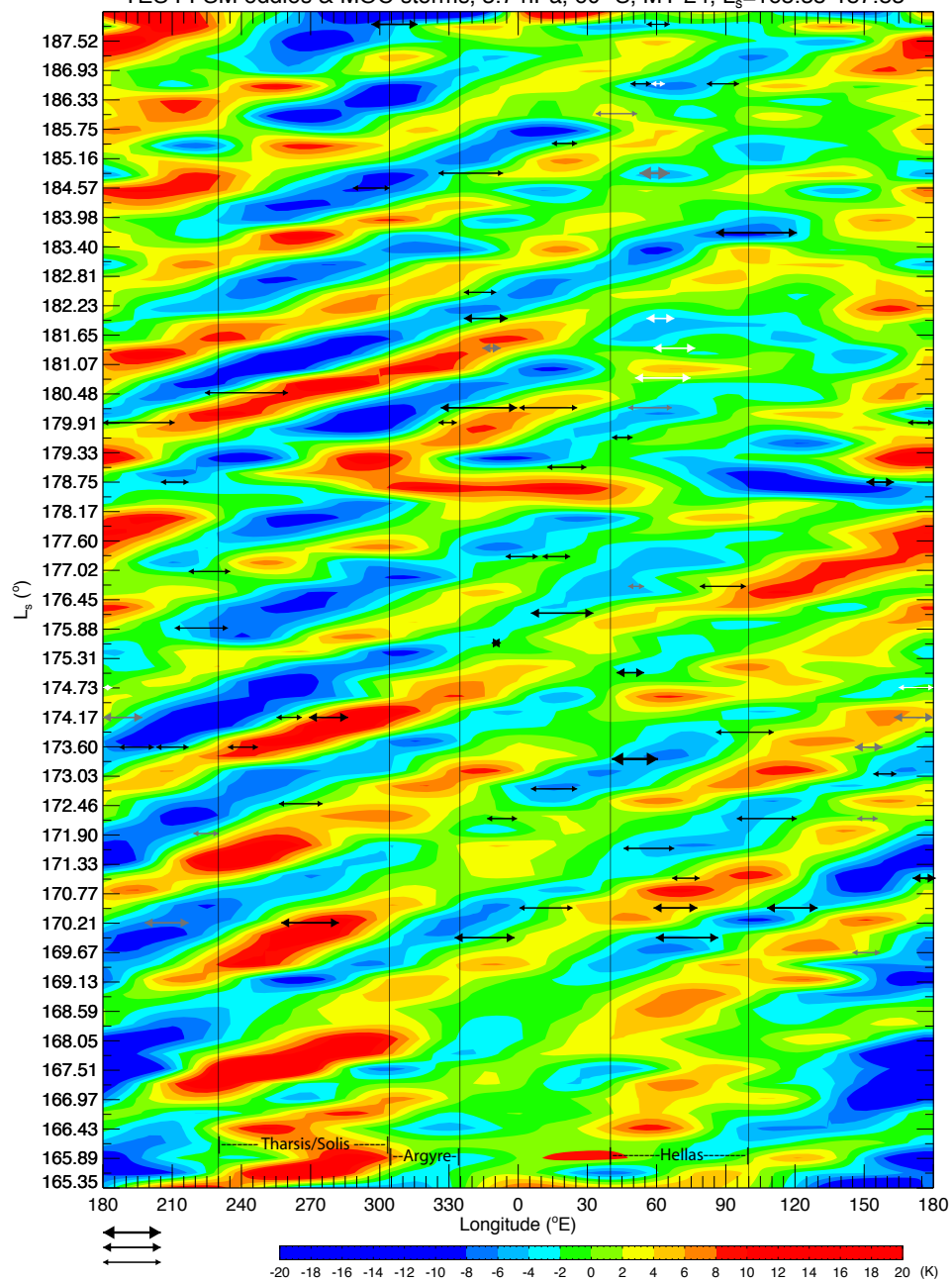
- Occasional northward progression

FFSM eddies and MOC storms, 60° S, 3.7 hPa, MY 25

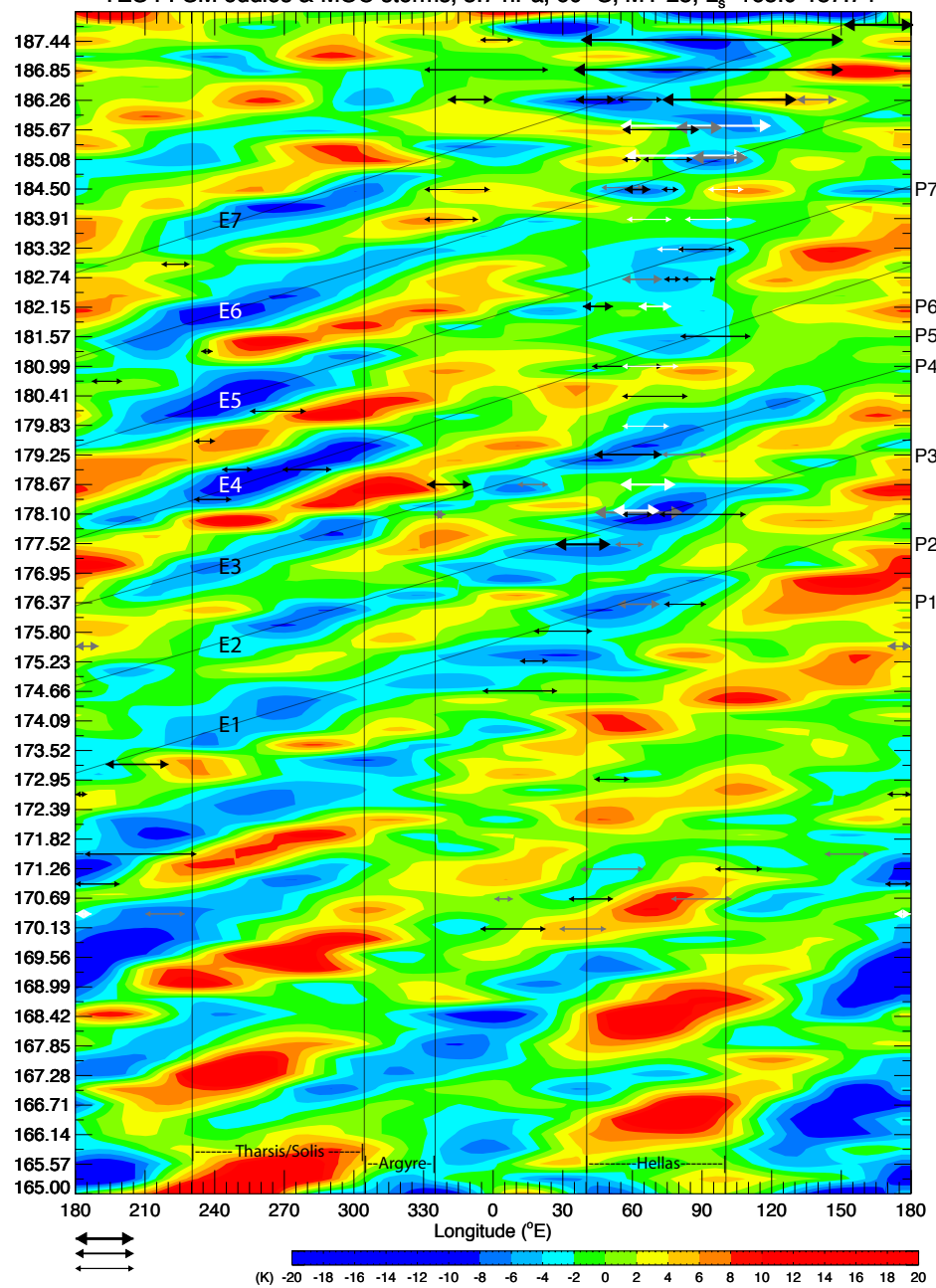


- Correlation between eastward propagation of cold anomalies and eastward evolution of storms.
 - Eastward trend is present in most of the sequences, particularly E1, 2, 3, 5, and 6
 - Northward trend is most notable as E2 and E5 pass through Hellas at $\sim L_s=178$ and 182° .

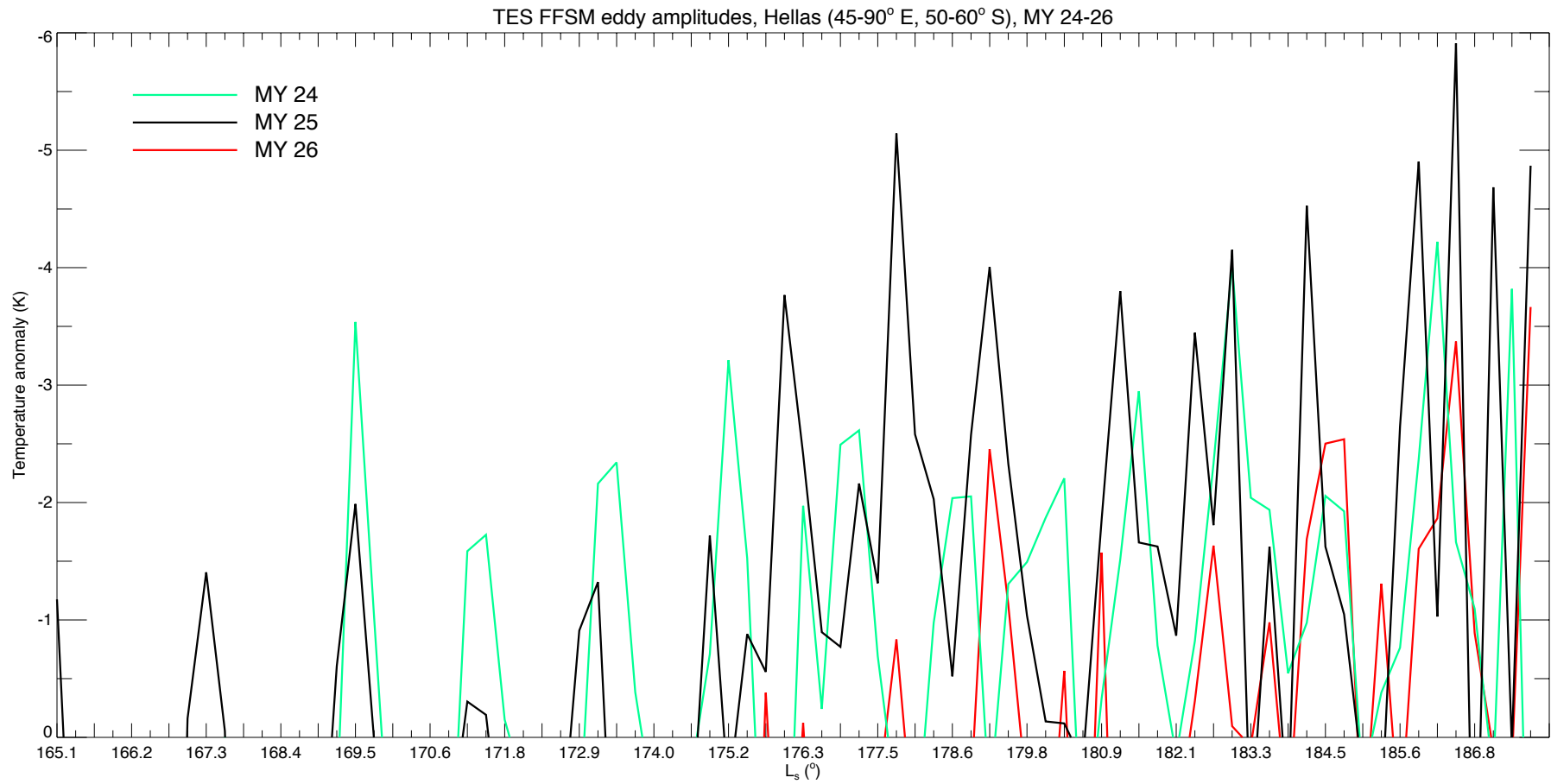
TES FFSM eddies & MOC storms, 3.7 hPa, 60° S, MY 24, $L_s=165.35-187.83^\circ$



TES FFSM eddies & MOC storms, 3.7 hPa, 60° S, MY 25, $L_s=165.0-187.74^\circ$



FFSM cold anomalies, Hellas, MY 24-26



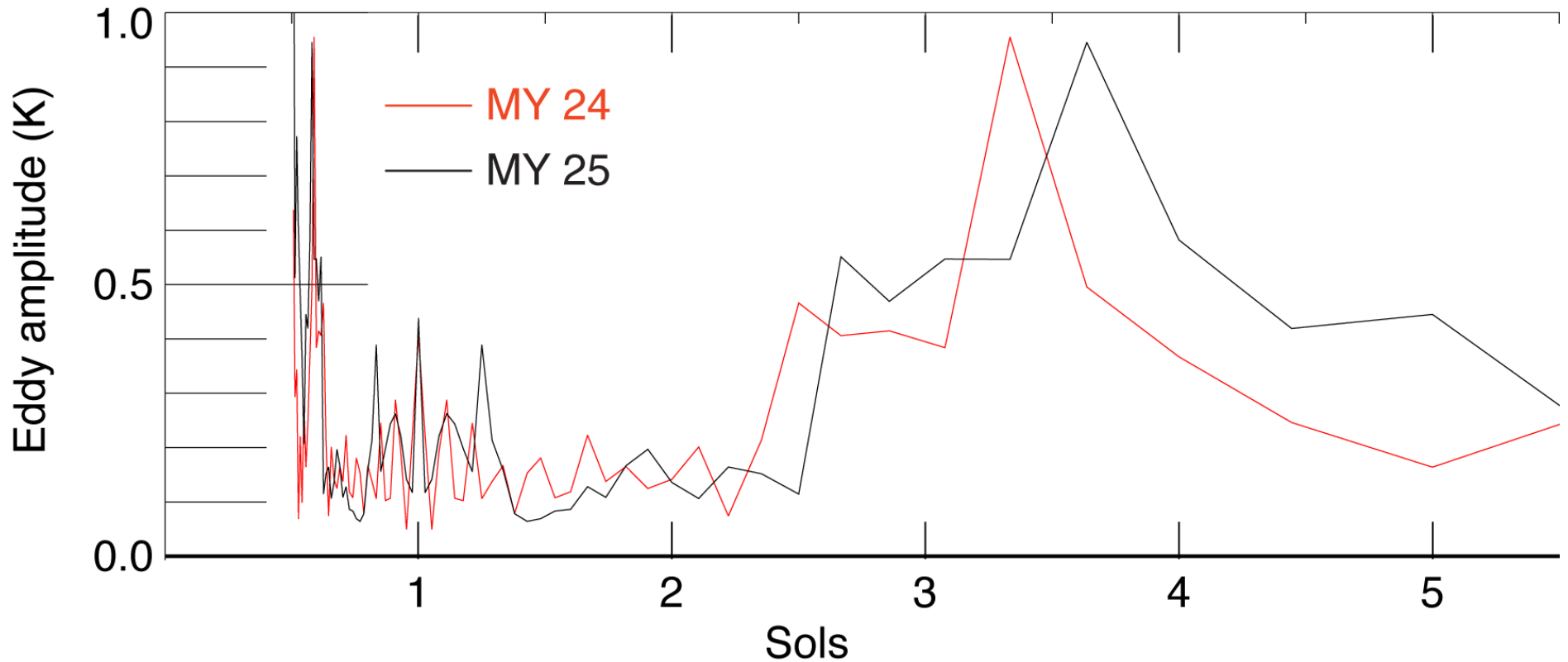
Phase & periodicity

- Phase speed calculation $c(x)=\Delta x/\Delta t$, where $\Delta x = (r_{eq} \cdot \cos\varphi) \cdot \Delta\lambda$, r_{eq} is planetary radius, φ latitude, λ longitude, and t time at 180° E.
- MY 24– 26 mean global phase speeds of 14.3, 13.8, 13.7 m s^{-1} respectively show that MY 25 eddies were $\sim 0.5 \text{ m s}^{-1}$ slower than those in MY 24.
- Mean eddy periodicity, P , in Hellas (60° E) was 2.7, 2.9, and 3.1 sols for MY 24–26 respectively

Table 1: Baroclinic eddy (global) phase speeds, c (m s^{-1}), and period, P (sols), at 60° E , MY 24–26

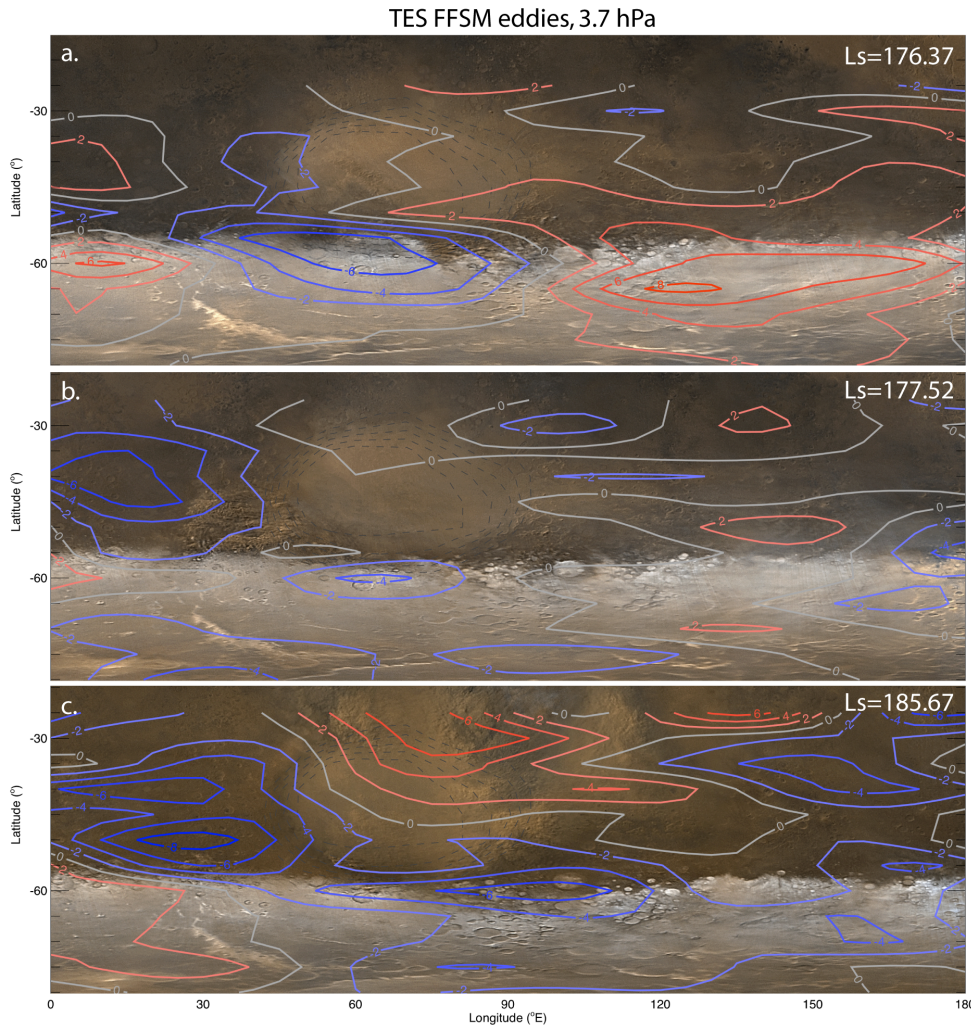
$\sim L_s$ ($^\circ$) eddy at 60° E	Eddy #	c MY24	c MY25	c MY26	P MY24	P MY25	P MY26
176.5	E1	12.8	13.8				
178.0	E2	13.4	14.5	15.6	2.7	2.8	
179.3	E3	14.1	14.8	14.3	2.6	2.5	2.8
181.0	E4	14.5	13.1	13.8	2.8	3.0	2.9
182.7	E5	15.2	13.5		2.7	2.9	
184.6	E6	16.0	13.8	12.9	2.5	2.8	
186.3	E7	13.8	13.2	11.8	2.9	3.3	3.7
	Mean	14.3	13.8	13.7	2.7	2.9	3.1

FFT power spectra of TES FFISM eddies, Hellas, MY 24 & 25



- dominant periodicity of ~ 3.5 sols; MY 25 longer
- moderately high adjacent amplitudes from 2.5-3 sols

FFSM Eddies and MOC storms, Hellas, MY 25



- Storms emerge on the leading edges of strong-amplitude cold centers
- Although a first order approximation would locate cold fronts between cold and warm FFSM anomalies, their location can not be determined from FFSM eddies alone. Pressure and wind data is also required.
- Limited vertical and longitudinal resolution of TES data, and subsequent 5° longitudinal resolution of FFSM eddy bins, precludes precise determination of cold fronts.
- Fronts are most intense close to the surface, however TES averaging of the lowest scale height reduces their signal.
- Furthermore, there is probably a phase shift between FFSM eddy and pressure fields, since isobaric and isosteric surfaces intersect under baroclinic conditions.

Interannual comparison

- MY 24–26 Hellas periodicities of 2.7, 2.9, and 3.1 sols respectively show minor interannual variability, as well as global phase speeds of 14.3, 13.8, and 13.7 m s⁻¹.
- The most notable difference is the amplitude of E1–E7 eddies in Hellas, with all seven MY 25 eddies colder than ~ -3.5 K, compared with two in MY 24 and one in MY 26.

Working Hypothesis

- Baroclinic eddies played a significant role in triggering the MY 25 precursor phase regional storms.
- It is possible that the sustained series of high-magnitude eddies in MY 25 was a factor in PDS interannual variability. There may be a critical eddy temperature threshold (< -3.5 K) exceeded in MY 25
- Constructive interference of transient eddies and other circulation components in MY 25, including sublimation flow, anabatic winds, diurnal tides, and dust-induced thermal tides, may have led to the initiation, amplification, and sustained expansion of precursor storms.
Constructive interference increases surface stresses capable of lifting dust. Dust suspended during the precursor phase greatly amplified thermal tides, that in turn contributed to greater storm growth within, and expansion out of Hellas, compared to other years.

PDS genesis

- If other interannual differences in transient eddy activity were involved in MY 25 PDS genesis, then they may be features undetectable by TES, such as very shallow disturbances.
- Non-dynamical factors possibly governing PDS interannual variability include dust sources and sinks.

Conclusions

Integration of FFSM and MOC MY 24 and 25 data shows interesting temporal and spatial associations between the evolution of eddies and storms, including:

- 1) comparable periodicities of travelling waves and pulses of storm activity;
- 2) concurrent eastward propagation of both eddies and storms;
 - Stronger correlation of eastward progression in MY 25
 - More northward propagation in MY 25
- 3) location of high-latitude storms on the leading (eastern) edge of eddies (cold anomalies)

These results suggest a causal relationship between baroclinic eddies and local storm initiation.

Future work

- Use GCM to decompose circulation components and assess their contribution to storm initiation and expansion
- Compare MY 26 FFISM and MOC data

References

- Barnes, J. R., 2001: Asynoptic fourier transform analyses of MGS TES data: Transient baroclinic eddies. *Bulletin of the American Astronomical Society*, **33**, 1088.
- Barnes, J. R., 2003: Mars Weather Systems and Maps: FFSM Analyses of MGS TES Temperature Data. *Sixth International Conference on Mars*, Pasadena, California, USA.
- Barnes, J. R., 2006: FFSM Studies of Transient Eddies in the MGS TES Temperature Data. *Mars Atmosphere Modelling and Observations*, Granada, Spain
- Cantor, B., 2007: MOC observations of the 2001 Mars planet-encircling dust storm. *Icarus*, **186**, 60-96.